Pharm Res (2013) 30:1574–1585
DOI 10.1007/s11095-013-0996-5

RESEARCH PAPER

The Antitumor Effect of a New Docetaxel-Loaded Microbubble Combined with Low-Frequency Ultrasound *In Vitro*: Preparation and Parameter Analysis

Shu-Ting Ren • Yi-Ran Liao • Xiao-Ning Kang • Yi-Ping Li • Hui Zhang • Hong Ai • Qiang Sun • Jing Jing • Xing-Hua Zhao • Li-Fang Tan • Xin-Liang Shen • Bing Wang

Received: 27 August 2012 / Accepted: 28 January 2013 / Published online: 16 February 2013
© Springer Science+Business Media New York 2013

ABSTRACT

Purpose To develop a novel docetaxel (DOC)-loaded lipid microbubbles (MBs) for achieving target therapy and overcoming the poor water-solubility drawback of DOC.

Methods A novel DOC-loaded microbubble (DOC + MB) was prepared by lyophilization and the physicochemical properties including ultrasound contrast imaging of the liver were measured. The anti-tumor effect of the DOC + MBs combined with low-frequency ultrasound (LFUS; 0.8Hz, 2.56 W/cm^2, 50% cycle duty) on the DLD-1 cancer cell line was examined using an MTT assay.

Results The physicochemical properties of the two tested formats of DOC + MBs (1.0 mg and 1.6 mg) was shown: concentration, $(6.74 \pm 0.02) \times 10^8$ bubbles/mL and $(8.27 \pm 0.15) \times 10^8$ bubbles/mL; mean size, 3.296 ± 0.004 μm and 3.387 ± 0.005 μm; pH value, 6.67 ± 0.11 and 6.56 ± 0.05; release rate, 3.41% and 12.50%; Zeta potential, -37.95 ± 7.84 mV and -44.35 ± 8.70 mV; and encapsulation efficiency, 54.9 ± 6.21% and 46.3 ± 5.69%, respectively. Compared with SonoVue, the DOC + MBs similarly enhanced the echo signal of the liver imaging. The antitumor effect of the DOC + MBs/LFUS group was significantly better than that of DOC alone and that of the normal MBs/LFUS groups.

Conclusions The self-made DOC + MBs have potential as a new ultrasound contrast agent and drug-loaded microbubble, and can obviously enhance the antitumor effect of DOC under LFUS exposure.

KEY WORDS docetaxel · lipid microbubbles · tumor-targeted therapy · ultrasound contrast agent

ABBREVIATIONS

DOC	docetaxel
DOC + MB	docetaxel-loaded microbubble
IR	inhibitory rate
LFUS	low-frequency ultrasound
MB	microbubble
NMB	normal microbubble
NS	normal saline
PTX	paclitaxel
PBS	phosphate buffer saline
RP-HPLC	reverse-phase liquid chromatography
TtoPk	time to peak
TIC	time intensity curve
UCA	ultrasound contrast agent
US	ultrasound

INTRODUCTION

The World Environment Organization reported that cancer is now the leading cause of death in China (1), which lends

Shu-Ting Ren and Yi-Ran Liao contributed equally to this work.

S.-T. Ren • X.-N. Kang • J. Jing • B. Wang (✉)
Department of Pathology and Therapeutic Vaccines Engineering Center of Shaanxi Province, School of Medicine, Xi'an Jiaotong University, Xi'an 710061, China
e-mail: wangbing@mail.xjtu.edu.cn

Y.-R. Liao • Y.-P. Li • H. Zhang • Q. Sun • X.-H. Zhao
Department of Pharmacology and Therapeutic Vaccines Engineering Center of Shaanxi Province, School of Medicine, Xi'an Jiaotong University, Xi'an 710061, China

H. Ai • L.-F. Tan
Department of Ultrasound Imaging, First Affiliated Hospital of Medical College, Xi'an Jiaotong University, Xi'an 710061, China

X.-L. Shen
China National Biotechnology Group, Beijing 100029, China

urgency to the search for an effective cure for cancer patients. Chemotherapy remains the major treatment option for cancer patients, despite the development of various new therapeutic innovations such as immune and gene therapy (2,3). However, an issue with the available tumor chemotherapy is the inability to maximize the cytotoxic drug efficacy to kill most tumor cells while minimizing side effects, especially for strongly cytotoxic chemotherapy drugs such as paclitaxel (PTX), doxorubicin, vinorelbine and gemcitabine (4,5). To date, many studies have explored drug delivery techniques, which provide targeted-release of the chemotherapy drug to tumor tissues while reducing the side effects of the drugs (6,7).

Over the last few decades, scientists have explored effective drug delivery systems for chemotherapy drugs, including liposomes, parenteral emulsions, microparticles, microcapsules, and the use of prodrugs (8–13). Recently, microbubble (MB), which is ultrasound contrast agent (UCA), has undergone a rapid development for use as a drug delivery system (14–16). Compared with other drug delivery systems, the use of MBs to carry drugs and subsequent drug delivery using ultrasound (US) has many advantages. First, the MBs will rupture to release the drug in the targeted tissues upon exposure of the ultrasound wave (17). Second, the cavitation, shock-wave, and microjet produced by the MBs combined with US can temporarily perforate cell membranes and induce intracellular delivery of the drugs (18,19). Third, lipid MBs, which are coated by phospholipids, are favorable for encapsulating lipophilic drugs (20). Finally, the application of MBs combined with US can increase the permeability of blood vessels, which allows the drug to cross the vascular wall and enter into target organs or tissues. Therefore, MBs are a potential drug delivery system for chemotherapy and other drugs (3,21).

Docetaxel (DOC) is currently approved for therapy of breast and ovarian cancers (22), and it has also been found effective against head and neck cancers as well as non-small cell lung carcinomas (19,23). Thus, it is widely used in clinics due to its excellent anti-tumor effects (24,25). However, DOC is a highly hydrophobic molecule (19,20) and must be solubilized in tween-80, which causes hemolysis and other allergies in patients. This drawback led to our concept to encapsulate DOC in lipid MBs, which would improve DOC solubility by avoiding the use of tween-80 and providing DOC-targeted delivery to cancer tissue, while minimizing the dosage and the side-effect of the drug through systemic administration and maximizing its therapeutic benefit upon US exposure.

To support our hypothesis, we prepared a new DOC-loaded lipid microbubble. We then evaluated their physicochemical parameters. Furthermore, the anti-tumor effects of the DOC-loaded MBs were explored *in vitro*.

MATERIALS AND METHODS

Materials

Tert-butyl alcohol was purchased from Reagent Factory of Xi'an (Xi'an, China). As the components of the lipid MBs' shell, two phospholipids of dipalmitoylphosphatidylglycerol (Sodium Salt) (DPPG-Na) and distearoyl phosphatidylcholine (DSPC) were respectively purchased from Avanti Polar Lipids (Alabaster, AL, USA) and Shearwater Polymers (Huntsville, AL, USA). Palmitic acid was obtainted from Reagent Factory of Tianjing (Tianjing, China) and polyethylene plycol 4000 (PEG4000) was obtainted from Hercules (CA, USA). DOC was purchased from Knowshine Pharmachemicals Inc. (Shanghai, China). The SF6 (pressure, 101 kPa) as the inner gas phase of the MBs was purchased from Liming Chemical Industry Institute (Luoyang, China).

Preparation of DOC-Loaded MBs (DOC + MBs) and Normal Microbubbles

Normal microbubbles (NMBs), with no drug loaded, were prepared according to the method described previously (26). Two DOC + MBs formats, containing 1.0 mg and 1.6 mg DOC, were prepared according to the procedure used for the preparation of the NMBs, with slight modifications (Fig. 1). In brief, a mother liquid was prepared by mixing tert butyl alcohol and purified water, and certain amount of DPPG-Na and DSPC were subsequently dissolved into the mother liquid to prepare the phospholipids mixture. Then palmitic acid was suspended into the phospholipids mixture. Meanwhile, the appropriate amount of DOC was weighted and directly dissolved in tert butyl alcohol to prepare the solution of DOC. Then the solution of DOC and PEG4000 were suspended into the previous phospholipids mixture and stirred for 20 mins. The last mixtures of 1 mL were equally transferred into each 10 mL-cylindroid vial, and then lyophilized by freezer dryer (Peijing Boyikang Ltd. Co., Peijing, China). The SF6 was added after the lyophilization. Finally, the vials were sterilized by irradiation of Cobalt 60 after lidding. The MBs were reconstructed by the addition of 5 mL normal saline (NS) (Shaanxi Shenghua Pharmaceutical Co., Ltd.) through the vial plug, followed by hand agitation.

Detection of the Physicochemical Properties of the NMBs and DOC + MBs

The concentration and size distribution of the two DOC + MB formats were determined via methods similar to those previously reported using a Coulter counter device (Beckman Coulter Multisizer 3 3.51; Fullerton, CA, USA) (aperture diameter: 50 μm) (26). The Zeta potential and

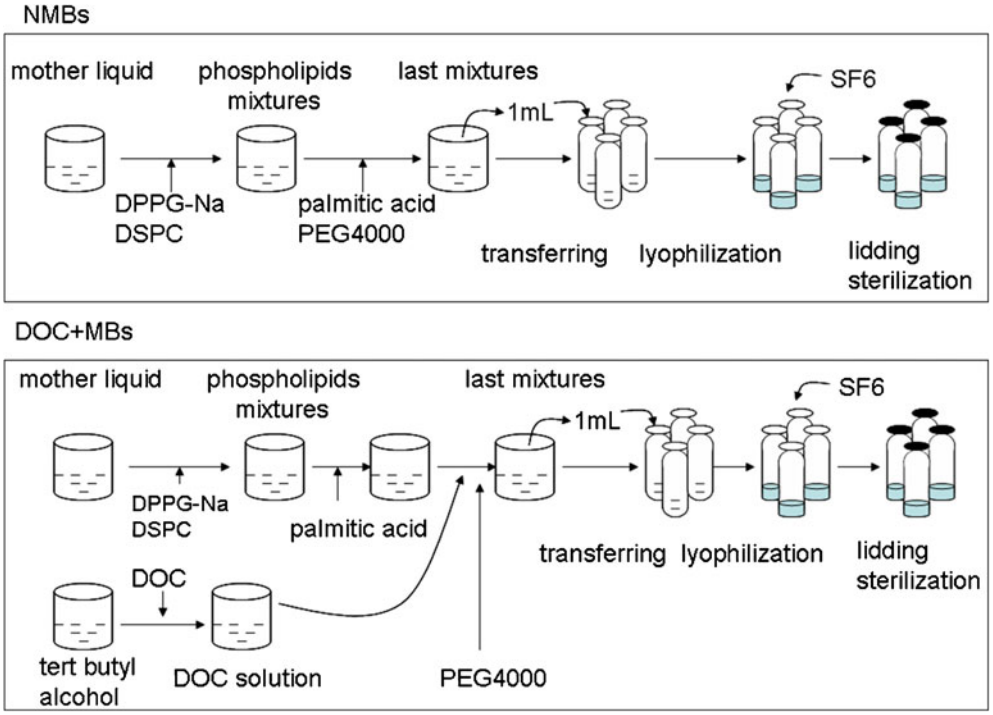

Fig. 1 The flow chart of NMBs' (*up*) and DOC + MBs'(*down*) preparation.

polydispersity index of the MBs were determined using a Malvern laser particle size analyzer (British Malvern Instruments Ltd.). The pH values of the MB suspensions were determined using a pH meter (PHS-3C + meter; Fangzhou Technology Ltd. Co., Beijing, China). Finally, the morphology of the MBs was observed using an optical microscope (Eclipse E100; Nikon, Tokyo, Japan).

Time-Dependent Stability of the NMBs and DOC + MBs in pH7.4 Phosphate Buffer Saline (PBS) at Body Temperature (37°C)

After the detection of their physicochemical properties, half milliliter of the NMBs and two formats DOC + MBs suspensions were respectively transferred into 5-mL eppendorf tube and diluted by 2.5 mL PBS with pH = 7.4. Then these MBs suspensions were placed in a 37°C water bath for 30 mins, 1 h, 2 h, 4 h and 6 h, respectively. According to the method described above, the size, Zetal potential and concentration of the MBs were finally measured again.

The Encapsulation Efficiency and Drug Release of the DOC + MBs Induced Via Low-Frequency Ultrasound (LFUS)

The encapsulation efficiency and drug release of the DOC + MBs were measured using reverse-phase liquid chromatography (RP-HPLC; Dalian Elite Analytical Instruments Co., Ltd, Dalian, China) and calculated using the following formulas: encapsulation efficiency = (total DOC-free DOC)/total DOC × 100%, drug release = DOC in the sediments after LFUS exposure-DOC in the sediments without LFUS exposure. In brife, 1.5 mL DOC + MBs suspension was diluted by an equal volume NS in a 15 mL-centrifuge tube and centrifuged for 5 mins at 1,368 g until the MBs gathered on the surface of the solution. Then these separated MBs were taken out into another 15 mL-centrifuge tube to dilute with an equal volume NS and repeat the centrifuge procedure again (One sample should repeat the above steps for three times). Finally, the sediments on the bottom of the three tubes were collected together to a 10 mL-vial and dissolved in 5 mL methly alcohol (Guangdong Guanghua Chemical Factor Co., Ltd. China). Then the amount of free DOC in the sediments was determined in triplicate by the RP-HPLC. For HPLC analysis, a reverse-phase SinoChrom ODS-BP column (200 × 4.6 mm i.d., pore size 5 μm, Dalian Elite Analytical Instruments Co., Ltd., China). The mobile phase of methanol/acetonitrile/water (50:30:20, v/v) was delivered at a flow rate 1 mL/min (Dalian Elite Analytical Instruments Co., Ltd., China) and DOC was quantified by UV absorbance (λ = 230 nm, Dalian Elite Analytical Instruments Co., Ltd., China). The area under the curve was integrated and the DOC concentration was calculated based on a linear calibration curve. Similarly, 1.5 mL MBs suspension was placed in the 12-well plate and exposured by the LFUS (0.8 MHz, 2.56 W/cm^2, 50%cycle duty) for 10 mins. Then the above same procedures repeated and the DOC in the sediments after LFUS exposure was obtained to calculate the drug release of the DOC + MBs. Finally, the release rate of the drug was determined by the formula: the release rate of the drug = released DOC/encapsulated DOC × 100%.

Ultrasound Contrast Imaging of the NMBs and DOC + MBs in the Liver of Dogs and Comparison with SonoVue

Animal Preparation

The study was approved by the Ethical Committee of Xi'an Jiaotong University and complied with the Practice Guidelines for Laboratory Animals of China. Two healthy dogs, weighing approximately 15 Kg each, underwent general anesthesia via intramuscular injection with Sumianxin (a compound of haloperidol, di toluidine thiazole and DHM99, 0.1 mL/Kg, Academy of Military Medicine Veterinary Research Institute, Changchun, China). Next, 3 mL of a pentobarbital sodium (3%) was administered via intramuscular injection.

Ultrasound Imaging of the Liver

The anesthetized dogs were placed on beds, and an area on the abdomen was prepared by the removal of all hair with shears. The transducer of a Diagnostic Ultrasound (Logiq 9 Digital Premium Ultrasound System, GE, USA) was fixed at the position of the liver while the solution of the UCA including NMBs, 1.6 mg of DOC + MBs and SonoVue (Bracco Imaging B.V. 31, Chemin de la Galaise, 1228, Plan-Les-Ouates Genève, Switzerland) were prepared. Next, 2.3 mL solution of SonoVue, the NMBs or 1.6 mg of DOC + MBs was administered subsequently via a bolus injection; after each UCA injection, the same volume of NS was administered. The detection of these UCA via US imaging was initiating during the UCA bolus injection. The average interval between the different UCA injections was at least 30 mins to ensure that the MBs of the previous UCA were cleared via metabolism. The US contrast imaging and the associated data were collected with the software provided with Logiq 9 Digital Premium Ultrasound System.

The Effect of the DOC + MBs Combined with LFUS on DLD-1 Cell Growth *in Vitro*

Cell Culture

DLD-1 cells, a human colon adenocarcinoma cell line, were obtained from the Biological Medical Research Center of Xi'an Jiaotong University and were cultured in RPMI 1640 medium (Thermo Fisher Biochemical Products Co., Ltd., Beijing, China) supplemented with 10% fetal bovine serum (FBS; Thermo Fisher Biochemical Products Co., Ltd., Beijing, China), penicillin (100 U/mL, Sigma Biochemical Products Co., Ltd.) and streptomycin (100 mg/mL, Sigma Biochemical Products Co., Ltd.) at 37°C in a humid incubator containing 5% CO_2 (Thermo Fisher Scientific Co., Ltd., Shanghai, China).

Grouping and Treatment

The DLD-1 cells were seeded in 12-well plates (Dow Corning Co., Ltd., USA). After 24 h, the cells were divided into six groups: control, DMSO (Guangdong Guanghua Chemical Factor Co., Ltd., China), DOC with LFUS (DOC/LFUS), NMBs with LFUS (NMBs/LFUS), DOC + MBs with LFUS (DOC + MBs/LFUS) and DOC alone. The appropriate quantities of DOC were dissolved in DMSO because of their poor solubility in water, and the final solution of DOC was prepared. Next, the DOC + MB and NMB suspensions were prepared (6.5×10^7 bubbles/mL final concentration of the MBs), and DOC was added to the wells of the different groups as appropriate, except for the no treatment control group. The DOC concentration (6 nmol/mL final concentration) was the same for the DOC alone, DOC/LFUS and DOC + MBs/LFUS groups. The total final volume of the different solutions added was the same in every well; 4 μL of DMSO was added to each well for the DMSO group. Meanwhile, the DOC/LFUS, NMBs/LFUS and DOC + MBs/LFUS groups underwent treatment with LFUS. Briefly, ultrasound irradiation was performed at a frequency of 0.8 MHz and an intensity of 2.56 W/cm^2 for 10 mins at 50% cycle duty using a commercial therapeutic US device (Dongjian Company, China; ultrasonic probe area: 2.8 cm^2). At 24 h after LFUS treatment, cell viability was measured using an MTT kit (Sigma Biochemical Products Co.,Ltd.). Next, the inhibitory rate (IR) of cellular growth was calculated according to the following formula: IR (%)=(the mean OD $_{\text{control group}}$-the mean OD $_{\text{treatment group}}$)/the mean OD $_{\text{control group}}$. The morphology of the cells was observed using a light microscope following Wright staining.

Statistical Analysis

An analysis of variance (GraphPad Prism 5.0 software) was used to assess the effects on the proliferation of the cells. $P<0.05$ was considered statistically significant.

RESULTS

The Physicochemical Properties of NMBs and DOC + MBs

The appearances of the NMBs and the two DOC + MBs suspensions were similar to that of the previously reported tPA-loaded MBs (26); however, the DOC + MBs suspensions appeared whiter than the NMBs and tPA-loaded MBs. Under the light microscope, the NMBs and DOC + MBs

were clustered as round spheres with smooth surfaces and varying sizes, and the centers of the spheres appeared empty and bright (Fig. 2). The concentrations of the two DOC + MBs formats (1.0 mg and 1.6 mg) were $(6.74\pm0.02)\times10^8$ bubbles/mL and $(8.27\pm0.15)\times10^8$ bubbles/mL, respectively, which were appropriately twice the concentration of the NMBs [$(4.67\pm0.02)\times10^8$ bubbles/mL)] and slightly higher than the SonoVue concentration (1 to 5×10^8 bubbles/mL) (27). The mean sizes of the MBs were 3.093 ± 0.004 μm for the NMBs, 3.296 ± 0.004 μm for the 1.0 mg DOC + MBs and 3.387 ± 0.005 μm for the 1.6 mg DOC + MBs. These values were slightly larger than the mean size of the SonoVue MBs (~2.5 μm) (27). The diameter ranges of three prepared MBs were 1.0~6 μm (Fig. 3), but 90% MBs in size were less than 3.5 μm. The polydispersity indexs of three MBs were 0.3~0.8, which indicated their polydispersity were good. Their Zeta potentials and pH values are shown in Table I.

The encapsulation efficiencies of the two DOC + MB formats were $54.9\pm6.21\%$ (1.0 mg) and $46.3\pm5.69\%$ (1.6 mg). The drug release rates are shown in Table II. Importantly, because more drug was released from the 1.6 mg DOC + MBs after LFUS exposure, the 1.6 mg DOC + MBs was selected for the following experiments.

Time-Dependent Stability of the NMBs and DOC + MBs in PBS with pH7.4

From 0 min to 30 mins, we found the Zeta potential, the particle size, and concentration of three prepared MBs suspensions in pH7.4 PBS had no obviously changed (Fig. 4), which indicated they had good stability within 30 mins. However, the particle size of the MBs was decreased as well as the MBs' concentration increased when the time was prolonged to 6 h, but the Zeta potential had no significant change. And the polydispersity of three MBs were good, which their polydispersity indexs were less than 0.8 from 0 min to 6 h.

Liver Ultrasound Imaging of the MBs and SonoVue

The results demonstrated that the trend in liver contrast-enhancement imaging with the self-made MBs, including the NMBs and 1.6 mg DOC-loaded MBs, was similar to that observed with the SonoVue MBs (Fig. 5). After continuous contrast imaging of the liver in a dog following administration of one of the three MB solutions (NMBs, 1.6 mg DOC + MBs and SonoVue), the line, contour and branch of the intrahepatic vasculature were clearly present. The image of the hepatic artery was first enhanced with a tree branch appearance. Next, the smaller veins in the liver were enhanced such that the whole parenchyma of the liver was enhanced. Finally, the enhanced image degraded slightly with the decrease of MB concentrations due to the degradation of lipid coat *in vivo*. The time intensity curve (TIC) analysis for the three MBs (Fig. 6) showed their ultrasound contrast signals were all an increasing trend before 90 s and an decreasing trend after 90 s. The first infusion of the self-made MBs began at 4–8 s and the time to peak (TtoPk) (time from the first image frame to peak intensity frame) was about 45 s. However, with SonoVue, the first infusion began at 6 s, and the TtoPk was 56.094 s. After 90 s, the ultrasound contrast signals of the three MBs decreased in the liver but the residence time of the self-made MBs was longer than that of SonoVue (Table III).

The Effect of the DOC + MBs Combined with LFUS on DLD-1 Cell Proliferation *in Vitro*

The ability of the DOC + MB to inhibit tumor cell proliferation was determined via IR (Fig. 7). Compared with the control and DMSO groups, the IR in all of the treatment groups was significantly increased ($P<0.001$). Furthermore,

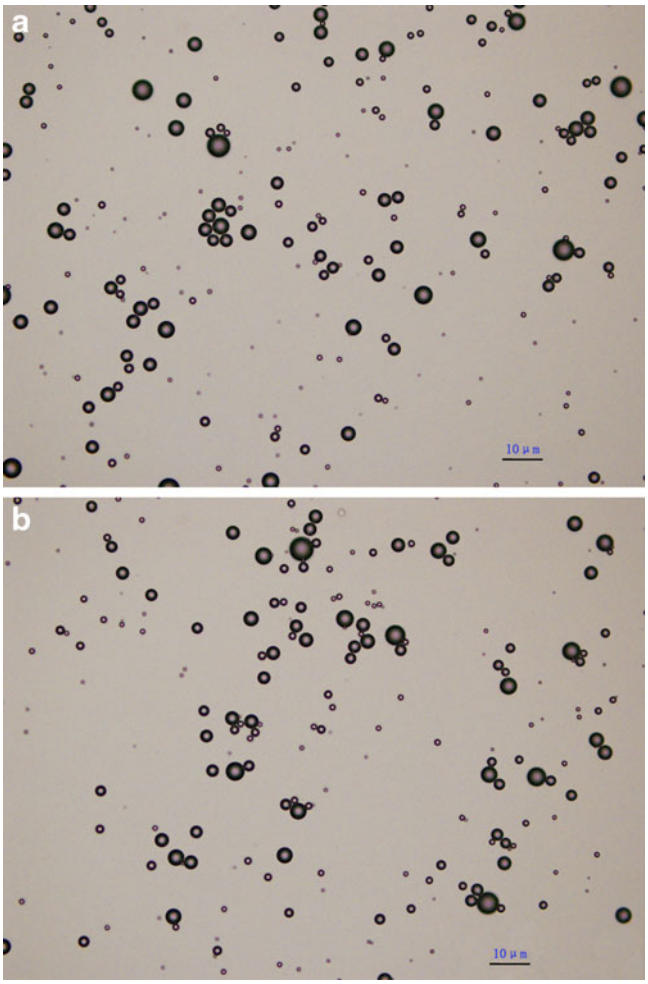

Fig. 2 The morphology of the DOC + MBs (**a**) and NMBs (**b**) using light microscopy (×200).

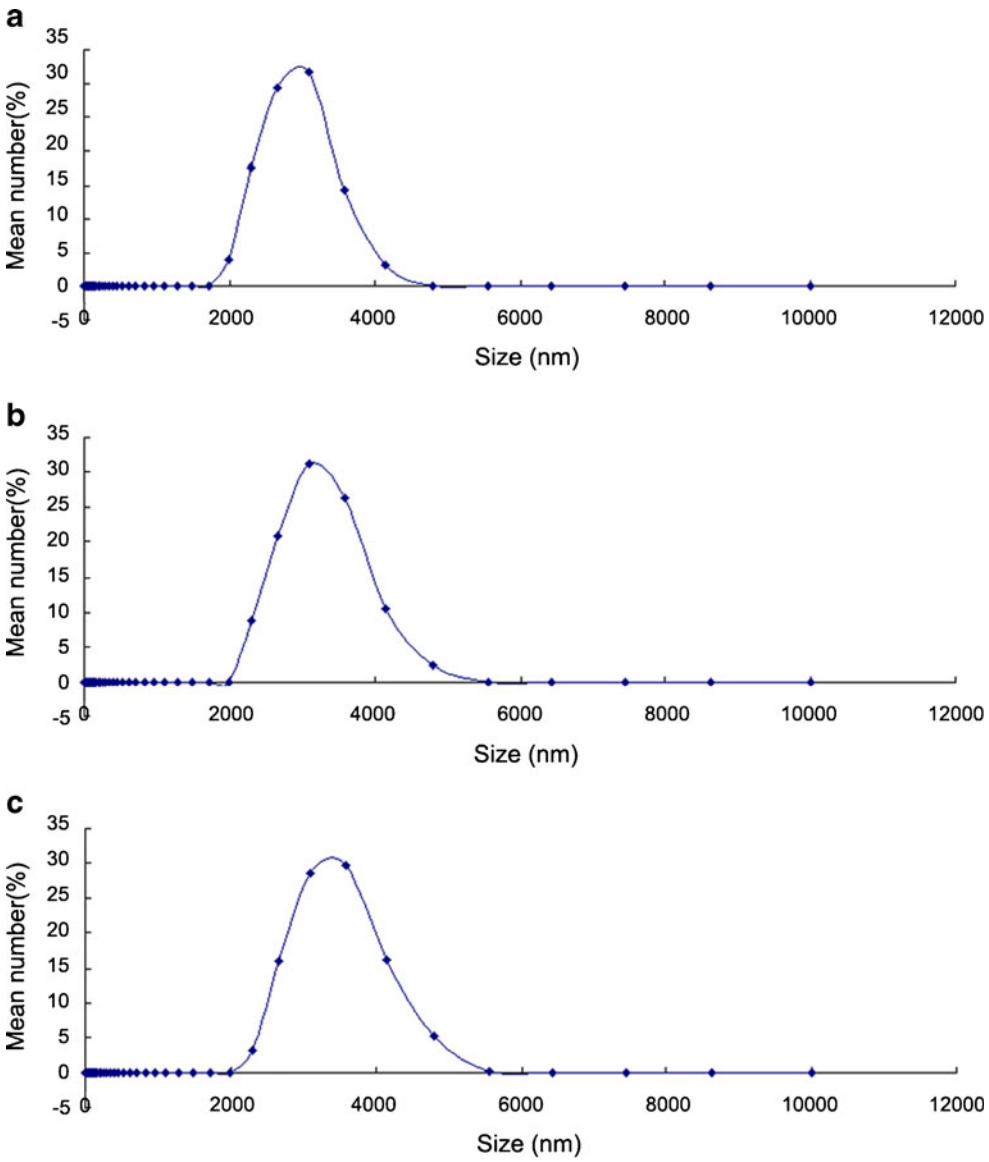

Fig. 3 The size distribution of the DOC + MBs and NMBs. (**a**) NMBs; (**b**) DOC + MBs (1.0 mg); (**c**) DOC + MBs (1.6 mg).

compared with DOC alone, DOC/LFUS and NMBs/LFUS, the IR in the DOC + MBs/LFUS group was significantly increased ($P<0.002$). Cells from select groups were observed for morphology after Wright staining. After treatment with NMBs/LFUS, DOC alone or DOC + MBs/LFUS, the growth of the DLD-1 cells was inhibited and the cellular intensity was lower than that in the control group (Fig. 8), particularly in the DOC + MBs/LFUS group. This result followed the same trends as those observed in the IR experiments.

DISCUSSION

Lipid shells have several advantages in maintaining the MBs' stability such as spontaneous self-assembly of a highly

Table I The Physicochemical Properties of the NMBs and DOC + MBs

	pH value	Zeta potential (mV)	Concentration ($\times 10^8$ bubbles/mL)	Particle size (μm)
NMBs	6.03 ± 0.12	−30.95 ± 1.76	4.67 ± 0.02	3.093 ± 0.004
DOC + MBs (1.0 mg)	6.67 ± 0.11	−37.95 ± 7.84	6.74 ± 0.02	3.296 ± 0.004
DOC + MBs (1.6 mg)	6.56 ± 0.05	−44.35 ± 8.70	8.27 ± 0.15	3.387 ± 0.005

Table II The Release of DOC from the Two DOC + MB Formats After LFUS Exposure

	Realease quantity (μg)	Release rate
DOC + MBs (1.0 mg)	2.04	3.41%
DOC + MBs (1.6 mg)	100.00	12.50%

oriented monolayer at the air-water interface, the low surface tension, high cohesiveness, and favorable ultrasound characteristics (28,29). Thus lipid-coated microbubbles are one of the most interesting and useful formulations used for biomedical imaging and drug delivery (28). Because DOC is a highly hydrophobic molecule and easy to dissolve with other lipid materials, lipid microbubbles could be chosen as drug delivery to make the DOC loaded into lipid microbubble shells. In this study, we prepared a new DOC-loaded lipid microbubble using a lyophilization method. The results showed that the encapsulation efficiency of the two DOC + MB formats was 54.9±6.21% and 46.3±5.69%, which was similar to the results reported by Kang J. and her collogues (5). It indicated the lipid microbubble can load the DOC as drug delivery. Although the rationale that DOC is encapsulted into lipid microbubbles is unclear in this study, we

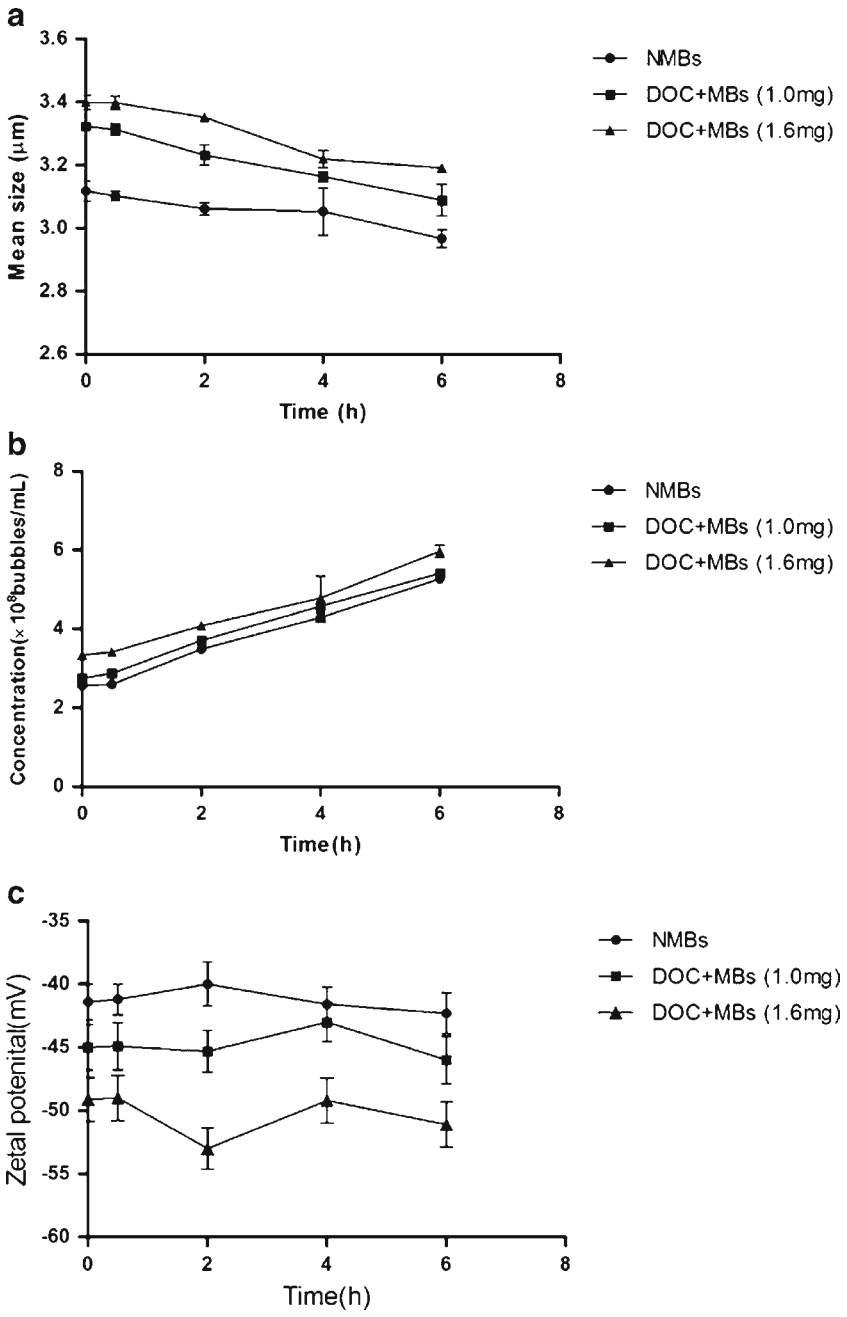

Fig. 4 Time-dependent changes of the NMBs' and DOC + MBs' mean size (**a**), concentration (**b**) and Zetal potential (**c**) in pH7.4 PBS.

thought it is mainly due to the high solubility of DOC in lipids reference to current studies (5,30,31).

However, it is well known that the size of MBs is an important factor for their clearance in the lung and for *in vivo* safety, as well as for the acoustic response of the MBs (32). Additionally, the size of MBs affects their distribution and pharmacodynamics after intravenous injection, bioeffects during US, gas-release profile and other related behaviors (33). Importantly, research has indicated that larger MBs produce a greater reduction in the proliferation of smooth muscle cells, but that the effective area of drug delivery and cell death is more closely controlled with smaller MBs (34). In this study, the mean size of the DOC-loaded lipid MBs was approximately 3 μm. Although it was larger than the diameter of the SonoVue MBs (2.5 μm) and the custmon-made DOC-loaded lipid MBs (623.1 nm) reported by Kang J. and her collogues (5), these DOC-loaded lipid MBs should be adaptable for intravenous administrations because the current accepted size of the MBs is in the 1–7 μm range, with an ideal size of 3 μm (14). And these DOC-loaded lipid MBs prepared by lyophilization were stored in the form of dry lyophilized power, which was superior to other lipid MBs in the form of aqueous prepared by the method of mechanical agitation or others (5,35). Meanwhile, their concentrations (4 to 8×10^8 bubbles/mL) were slightly higher than those of the SonoVue MBs (1 to 5×10^8 bubbles/mL) (27), and their pH values were close to 7.2, which is appropriate for standard intravenous administrations. Additionally, it had good polydispersity and size homogeneity as well as the stability of the MBs suspension in pH7.4 PBS within 30 mins at 37°C. Therefore, our self-made DOC + MBs not only have an appropriate particle size and concentration for use as UCAs but also have an appropriate particle size for use as a drug delivery agent.

The Zeta potential is an important characteristic of MB formulations and provides information on the colloidal dispersion stability, biological characteristics and drug-loading capacity of the MB formulations (36). In this study, the surface potential of three self-made MBs was negatively charged; however, the DOC + MBs had a more negative charge than the NMBs. It has been reported that the interactions between

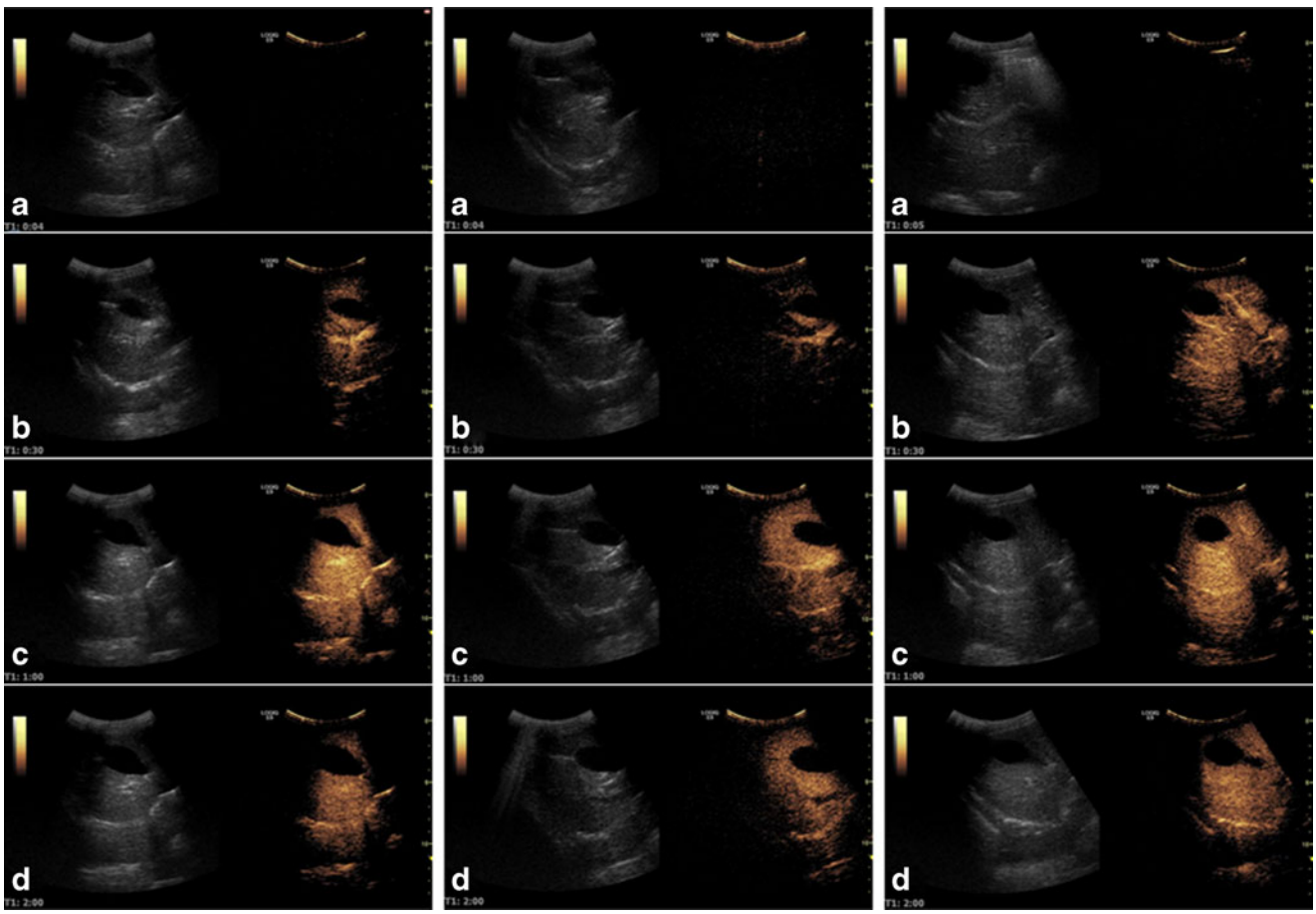

Fig. 5 Dynamic gray scale imaging of the liver before (*baseline*) or at different time points after the injection of SonoVue, NMBs or DOC + MBs. *Left*: SonoVue, *Middle*: NMBs, *Right*: DOC + MBs. (**a**) Baseline; (**b**, **c**, **d**): at 30 s, 60 s, and 120 s after injection, respectively. Four phases of liver imaging were present: baseline, arterial phase, portal phase and final phase.

the MBs and the capillary endothelium, as well as the resulting microcirculatory behavior, are Zeta potential dependent (36). Thus, longer capillary retention times for the anionic MBs in the myocardium and lung were observed (36). Therefore, it can be inferred that the DOC + MBs would have a better potency for lung carcinoma than for other organs.

We further explored the acoustic imaging characteristics of the MBs *in vivo* in the liver of dogs. After the intravenous injection of each the MBs, the results demonstrated three observable phases (arterial phase, portal phase and final phase) with strong image enhancement, particularly in the early arterial phase for the hepatic artery, which is not generally present following conventional ultrasound, and in the following portal phase. And there were no dog death during the contrast imaging. These results indicated that these self-made MBs are able to effectively enhance the color Doppler signal to help display the small blood vessels and safe, which is similar to the characteristics of SonoVue; thus, these self-made MBs have potential as a new ultrasound contrast agent. However, we found that the infusion time and TtoPk of the self-made MBs was earlier than that of the SonoVue, while their elimination time from the blood was longer. We hypothesized that this delay may be due to different injection speeds or concentration differences of the MBs used because the residence time of the self-made MBs was longer at higher concentrations. In this study, the total volume of the solution of both self-made MBs and SonoVue injected through the vein was the same, but their concentrations were slightly different, as described above. Additionaly, the difference of these UCAs in ultrasound contrast imaging may be caused by their different Zeta potential. The recent study manifested lipid microbubbles with a net negative charge can be retained within capillaries via complement-mediated attachment to endothelium which this property may be useful for the development of UCAs that can be imaged late after venous injection (36).

Table III The Time at First Enhancement, TtoPk and Residence Time of Three UCAs

	Time at first enhancement (sec)	TtoPk (sec)	Residence time (min)
SonoVue	6	56.094	~6
NMBs	8	48.065	~10
DOC + MBs	4	41.297	~15

LFUS has a stronger penetration power than high frequency ultrasound and is easily able to rupture the MBs (37,38). However, the US could directly kill cancer cell by the mechanism of thermal effect and non-thermal (or cavitation or sonodynamic) effect. For example, high intensity focused US could induce the tumor tissue coagulate necrosis to achieve the tumor therapy due to the thermal effect of US (39). But low intensity US can induce cell killing even without significant temperature

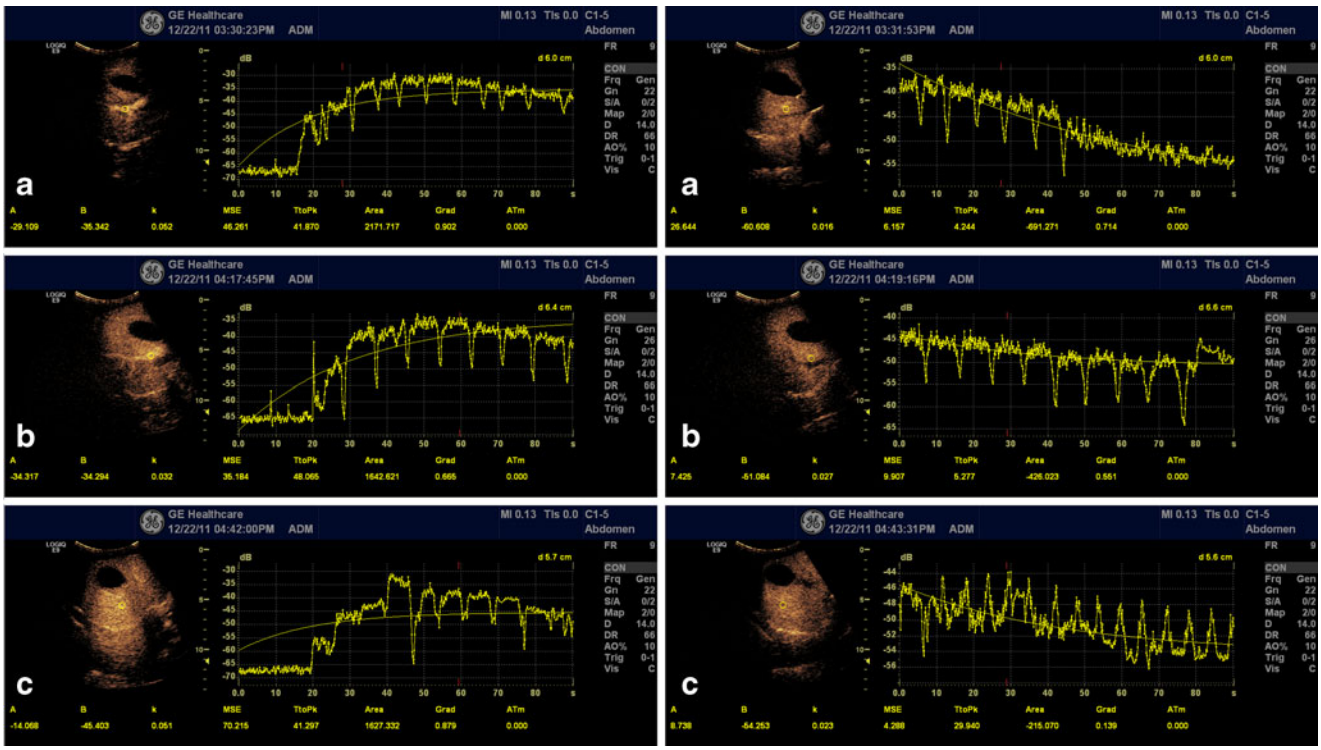

Fig. 6 TIC of the three MBs at different times. *Left*: The first 90 s, *Right*: After the first 90 s. (**a**) SonoVue, (**b**) NMBs, (**c**) DOC + MBs.

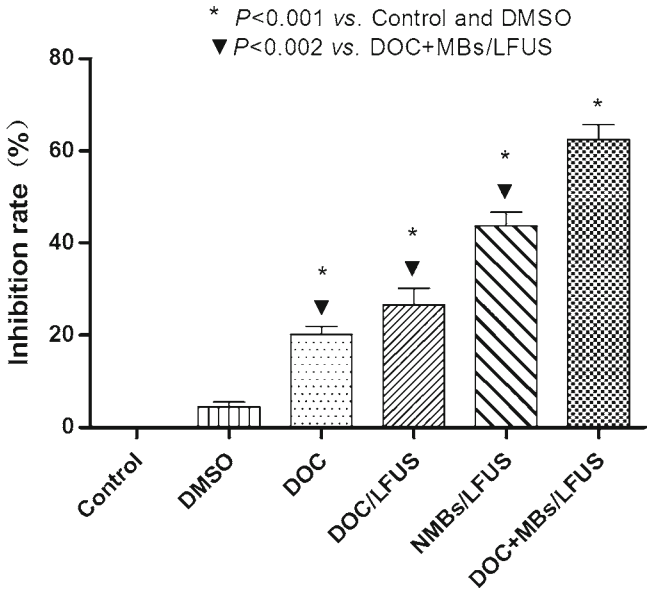

Fig. 7 The inhibitory rate of cell growth in different groups after treatment. * $P < 0.001$ *vs.* Control and DMSO; (*black down-pointing triangle*) $P < 0.002$ *vs.* DOC + MBs/LFUS.

rise and even at very low intensities (less than 0.5 W/cm^2), which is mainly mediated by the sonodynamic effect to induce apoptosis (40,41). The researches found lysis is commonly involved in US-induced cell killing *in vitro*, but *in vivo* it is less unlikely due to structural configurations of cells within the body. Therefore, although LFUS (20 kHz to 1 M) irradiation has the characteristic of penetrating into tissue easily with few sound energy absorption and little tissue damage (38), it could lysis cancer cells *in vitro*. Of course, the killing from a desired mode of cell death would be optimized by certain exposure parameters of US (such as US frequency, pulse repetition frequency, duty factor and intensity) (42). In order to eliminate the direct effect of LFUS on the tumor cell growth, we have previously explored the effect of different exposure parameters of LFUS (a frequence of 0.8 MHz) on three human tumor cell lines (MCF-7, SKOV3 and DLD-1) growth (Data not shown) and 0.8 MHz LFUS with an intensity of 2.56 W/cm^2 for 10 mins at 50% cycle duty was finally selected for use in the present study.

After LFUS exposure, the DOC in the two DOC + MB formats was partially released due to the rupture of the MBs; however, the release rate of the drug in following administration of 1.6 mg of DOC + MBs (12.5%) was higher than that following administration of 1.0 mg of DOC + MBs (3.6%). Thus, the amount of drug that entered the cells after the increased permeability caused by US cavitation was higher following administration of 1.6 mg of DOC + MBs. Therefore, 1.6 mg of DOC + MBs was selected to evaluate its pharmacological effect *in vitro*. The results of the MTT assay and the Wright staining showed that the inhibitory rate of tumor cell growth in the DOC + MBs/LFUS group was significantly higher than that in the DOC/LFUS, DOC alone and NMBs/LFUS groups. The DOC + MBs combined with LFUS were better at inhibiting tumor cell proliferation than DOC alone, which was consistent with the antitumor effect of the custom-made docetaxel-loaded lipid microbubble combined with US in inhibiting the growth of VX2 rabbit liver tumors *in vivo* (5). However, the effect of this DOC + MBs combined with LFUS on other tumor cell lines should be further confirmed.

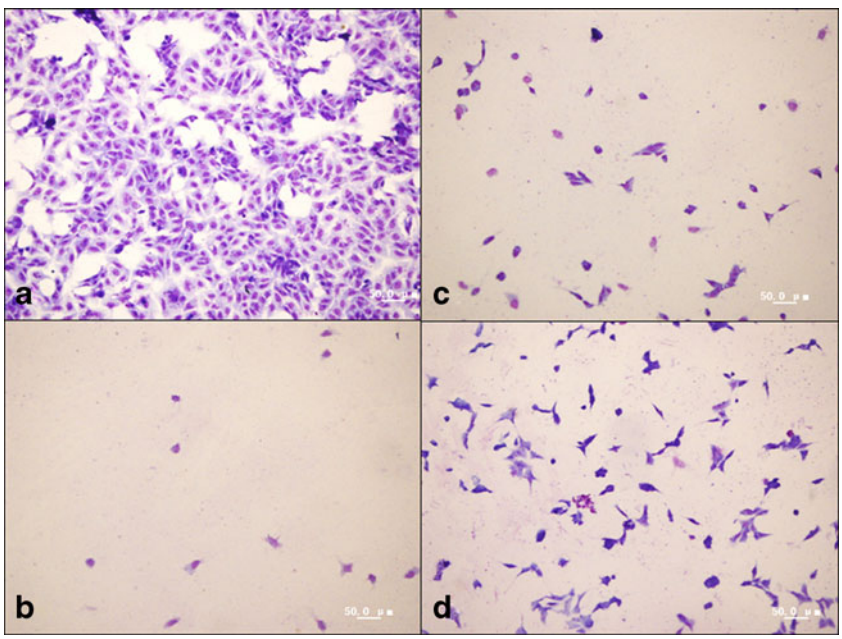

Fig. 8 The morphology of DLD-1 cells in some groups after treatment (Wright staining). (**a**) Control, (**b**) DOC + MBs/LFUS, (**c**) NMBs/LFUS, (**d**) DOC alone.

CONCLUSION

We have successfully prepared a new DOC + MB format that can enhance the ultrasound imaging of the liver as an UCA, and its combination with LFUS has a significant anti-tumor effect via increasing local drug delivery. However, the rationale underlying this study where DOC is encapsulted into lipid microbubbles and its ultrasound imaging property for other organs or some disease diagnosis should be explored and confirmed in future. And we will optimize the preparation of the DOC + MBs in an attempt to improve the encapsulation efficiency and minimize the bubble size. Furthermore, the *in vivo* anti-tumor effects of the DOC + MBs will be evaluated in future studies.

ACKNOWLEDGMENTS AND DISCLOSURES

The authors would like to thank Hua-Sheng Liu, Ph.D. and Jiang-Wei Liang for helps in the experiment. The present study was supported by the Scientific Technology Planning Foundation of Shaanxi Province (No.2010K12-01, 2011K12-56), Province Ministry Graveness Engineering Program (No.2009ZDKG-20; No.2008ZDKG-60, 2007ZDKG-290).

REFERENCES

1. Zhao P, Dai M, Chen W, Li N. Cancer trends in China. Jpn J Clin Oncol. 2010;40(4):281–5.
2. Baeuerle PA, Itin C. Clinical experience with gene therapy and bispecific antibodies for T cell-based therapy of cancer. Curr Pharm Biotechnol. 2012;13(8):1399–408.
3. Anwer K, Kao G, Proctor B, Anscombe I, Florack V, Earls R, *et al.* Ultrasound enhancement of cationic lipid-mediated gene transfer to primary tumors following systemic administration. Gene Ther. 2000;7(21):1833–9.
4. Yan F, Li X, Jin Q, Jiang C, Zhang Z, Ling T, *et al.* Therapeutic ultrasonic microbubbles carrying paclitaxel and LyP-1 peptide: preparation, characterization and application to ultrasound-assisted chemotherapy in breast cancer cells. Ultrasound Med Biol. 2011;37(5):768–79.
5. Kang J, Wu X, Wang Z, Ran H, Xu C, Wu J, *et al.* Antitumor effect of docetaxel-loaded lipid microbubbles combined with ultrasound-targeted microbubble activation on VX2 rabbit liver tumors. J Ultrasound Med. 2010;29(1):61–70.
6. Waite CL, Roth CM. Nanoscale drug delivery systems for enhanced drug penetration into solid tumors: current progress and opportunities. Crit Rev Biomed Eng. 2012;40(1):21–41.
7. Guarneri V, Dieci MV, Conte P. Enhancing intracellular taxane delivery: current role and perspectives of nanoparticle albumin-bound paclitaxel in the treatment of advanced breast cancer. Expert Opin Pharmacother. 2012;13(3):395–406.
8. Collins-Gold L, Lyons R, Bartholow L. Parenteral emulsions for drug delivery. Adv Drug Deliv Rev. 1990;5(3):189–208.
9. Harris JD, Gutierrez AA, Hurst HC, Sikora K, Lemoine NR. Gene therapy for cancer using tumour-specific prodrug activation. Gene Ther. 1994;1(3):170–5.
10. Kato T, Sato K, Sasaki R, Kakinuma H, Moriyama M. Targeted cancer chemotherapy with arterial microcapsule chemoembolization: review of 1013 patients. Cancer Chemother Pharmacol. 1996;37(4):289–96.
11. Luo G, Yu X, Jin C, Yang F, Fu D, Long J, *et al.* LyP-1-conjugated nanoparticles for targeting drug delivery to lymphatic metastatic tumors. Int J Pharm. 2010;385(1–2):150–6.
12. O'Shaughnessy JA. Pegylated liposomal doxorubicin in the treatment of breast cancer. Clin Breast Cancer. 2003;4(5):318–28.
13. Park JW. Liposome-based drug delivery in breast cancer treatment. Breast Cancer Res. 2002;4(3):95–9.
14. Schutt EG, Klein DH, Mattrey RM, Riess JG. Injectable microbubbles as contrast agents for diagnostic ultrasound imaging: the key role of perfluorochemicals. Angew Chem Int Ed. 2003;42(28):3218–35.
15. Tartis MS, McCallan J, Lum AFH, LaBell R, Stieger SM, Matsunaga TO, *et al.* Therapeutic effects of paclitaxel-containing ultrasound contrast agents. Ultrasound Med Biol. 2006;32(11):1771–80.
16. Zhou X, Qin H, Li J, Wang B, Wang C, Liu Y, *et al.* Platelet-targeted microbubbles inhibit re-occlusion after thrombolysis with transcutaneous ultrasound and microbubbles. Ultrasonics. 2011;51(3):270–4.
17. Lentacker I, De Smedt SC, Sanders NN. Drug loaded microbubble design for ultrasound triggered delivery. Soft Matter. 2009;5(11):2161–70.
18. Barnett S. Nonthermal issues: cavitation–its nature, detection and measurement. Ultrasound Med Biol. 1998;24:S11–21.
19. Liu Y, Miyoshi H, Nakamura M. Encapsulated ultrasound microbubbles: therapeutic application in drug/gene delivery. J Control Release. 2006;114(1):89–99.
20. Engels FK, Mathot RAA, Verweij J. Alternative drug formulations of docetaxel: a review. Anti Cancer Drugs. 2007;18(2):95.
21. Frenkel PA, Chen S, Thai T, Shohet RV, Grayburn PA. DNA-loaded albumin microbubbles enhance ultrasound-mediated transfection *in vitro*. Ultrasound Med Biol. 2002;28(6):817–22.
22. Michaud LB, Valero V, Hortobagyi G. Risks and benefits of taxanes in breast and ovarian cancer. Drug Saf. 2000;23(5):401–28.
23. Rowinsky EK, Donehower RC. Paclitaxel (taxol). N Engl J Med. 1995;332(15):1004.
24. Cortes JE, Pazdur R. Docetaxel. J Clin Oncol. 1995;13(10):2643–55.
25. Sanli UA, Uslu R, Karabulut B, Sezgin C, Saydam G, Omay SB, *et al.* Which dosing scheme is suitable for the taxanes? An *in vitro* model. Arch Pharm Res. 2002;25(4):550–5.
26. Ren ST, Zhang H, Wang YW, Jing BB, Li YX, Liao YR, *et al.* The preparation of a new self-made microbubble-loading urokinase and its thrombolysis combined with low-frequency ultrasound *in vitro*. Ultrasound Med Biol. 2011;37(11):1828–37.
27. Schneider M. Characteristics of SonoVuetrade mark. Echocardiography. 1999;16(7, Pt 2):743–6.
28. Sirsi S, Borden M. Microbubble compositions, properties and biomedical applications. Bubble Sci Eng Technol. 2009;1(1–2):3–17.
29. Duncan PB, Needham D. Test of the Epstein-Plesset model for gas microparticle dissolution in aqueous media: effect of surface tension and gas undersaturation in solution. Langmuir. 2004;20(7):2567–78.
30. Unger EC, McCreery TP, Sweitzer RH, Caldwell VE, Wu Y. Acoustically active lipospheres containing paclitaxel: a new therapeutic ultrasound contrast agent. Invest Radiol. 1998;33(12):886–92.
31. Cochran MC, Eisenbrey J, Ouma RO, Soulen M, Wheatley MA. Doxorubicin and paclitaxel loaded microbubbles for ultrasound triggered drug delivery. Int J Pharm. 2011;414(1–2):161–70.

32. Tinkov S, Bekeredjian R, Winter G, Coester C. Microbubbles as ultrasound triggered drug carriers. J Pharm Sci. 2009;98(6):1935–61.
33. Talu E, Hettiarachchi K, Zhao S, Powell RL, Lee AP, Longo ML, *et al.* Tailoring the size distribution of ultrasound contrast agents: possible method for improving sensitivity in molecular imaging. Mol Imaging. 2007;6(6):384–92.
34. Phillips LC, Klibanov AL, Wamhoff BR, Hossack JA, editors. Ultrasound-microbubble-mediated drug delivery efficacy and cell viability depend on microbubble radius and ultrasound frequency 2010: IEEE International Ultrasonics Symposium Proceedings.
35. Klibanov AL. Preparation of targeted microbubbles: ultrasound contrast agents for molecular imaging. Med Biol Eng Comput. 2009;47(8):875–82.
36. Fisher NG, Christiansen JP, Klibanov A, Taylor RP, Kaul S, Lindner JR. Influence of microbubble surface charge on capillary transit and myocardial contrast enhancement. J Am Coll Cardiol. 2002;40(4):811–9.
37. Wang B, Wang L, Zhou XB, Liu YM, Wang M, Qin H, *et al.* Thrombolysis effect of a novel targeted microbubble with low-frequency ultrasound *in vivo*. Thromb Haemost. 2008;100(2):356–61.
38. Daffertshofer M, Gass A, Ringleb P, Sitzer M, Sliwka U, Els T, *et al.* Transcranial low-frequency ultrasound-mediated thrombolysis in brain ischemia: increased risk of hemorrhage with combined ultrasound and tissue plasminogen activator: results of a phase II clinical trial. Stroke. 2005;36(7):1441–6.
39. Jenne JW, Preusser T, Gunther M. High-intensity focused ultrasound: principles, therapy guidance, simulations and applications. Z Med Phys. 2012 Aug 9.
40. Feril Jr LB, Kondo T. Biological effects of low intensity ultrasound: the mechanism involved, and its implications on therapy and on biosafety of ultrasound. J Radiat Res. 2004;45(4):479–89.
41. Feril Jr LB, Kondo T. Major factors involved in the inhibition of ultrasound-induced free radical production and cell killing by pre-sonication incubation or by high cell density. Ultrason Sonochem. 2005;12(5):353–7.
42. Tachibana K, Feril Jr LB, Ikeda-Dantsuji Y. Sonodynamic therapy. Ultrasonics. 2008;48(4):253–9.